

Closed-form Approximation for Performance Bound of Finite Blocklength Massive MIMO Transmission

Xiaohu You, *Fellow, IEEE*, Bin Sheng, Yongming Huang, *Senior Member, IEEE*, Wei Xu, *Senior Member, IEEE*, Chuan Zhang, *Senior Member, IEEE*, Dongming Wang, *Senior Member, IEEE*, Pengcheng Zhu, *Senior Member, IEEE*, Chen Ji

Abstract—Ultra-reliable low latency communications (uRLLC) is adopted in the fifth generation (5G) mobile networks to better support mission-critical applications that demand high level of reliability and low latency. With the aid of well-established multiple-input multiple-output (MIMO) information theory, uRLLC in the future 6G is expected to provide enhanced capability towards extreme connectivity. Since the latency constraint can be represented equivalently by blocklength, channel coding theory at finite blocklength plays an important role in the theoretic analysis of uRLLC. On the basis of Polyanskiy’s and Yang’s asymptotic results, we first derive the exact close-form expressions for the expectation and variance of channel dispersion. Then, the bound of average maximal achievable rate is given for massive MIMO systems in ideal independent and identically distributed fading channels. This is the study to reveal the underlying connections among the fundamental parameters in MIMO transmissions in a concise and complete close-form formula. Most importantly, the inversely proportional law observed therein implies that the latency can be further reduced at expense of spatial degrees of freedom.

Index Terms—Channel coding, finite blocklength, maximal achievable rate, MIMO, uRLLC

I. INTRODUCTION

IN the beyond fifth-generation (B5G) mobile communication network, ultra-reliable low latency communications (uRLLC) are designed to support a plethora of mission-critical applications, such as autonomous vehicles and virtual reality, where seamless and reliable data transmission is the key to the feasibility of service [1], [2]. The primary objective of uRLLC, as per the third-generation partnership project (3GPP), is to reduce the latency down to 1 ms and simultaneously guaranteeing reliability higher than 99.999% [3]. On the one hand, driven by the increasingly stringent requirements in the emerging application scenarios [4], further enhanced capability of uRLLC is expected towards 6G $TK\mu$ extreme connectivity [5], i.e., the latency is reduced from ms-level to μ s-level. On the other hand, new applications such as extended reality (XR) will dissolve the boundary between uRLLC and

This work is supported by the National R&D Program of China (2020YFB1806603).

X. You, B. Sheng, Y. Huang, W. Xu, C. Zhang, D. Wang and P. Zhuare with National Mobile Communications Research Laboratory, Southeast University, Nanjing 210096, China and Purple Mountain Laboratories, Nanjing 211111, China.

Chen Ji is with School of Information Science and Technology, Nantong University, Nantong 226019, China.

Corresponding author: X. You, B. Sheng (e-mail: xhyu@seu.edu.cn, sbdtt@seu.edu.cn).

enhanced mobile broadband (eMBB) [6]. As a result, while error control is conventionally achieved by implementing the hybrid automatic repeat request (HARQ) mechanism, the strict latency constraint in uRLLC excludes multiple retransmissions therein. Additionally, potential new features such as high data rate also pose considerable challenges to 6G uRLLC [7].

Implementing URLLC relies on short packet length and short transmission time interval, which make channel estimation in URLLC more challenging. The authors in [8] propose a pilot-assisted channel estimation scheme in massive MIMO systems, which decreases channel estimation frequencies and computational latency overhead by utilizing block-fading channel property. With limited training and feedback overheads, joint uplink and downlink URLLC transmission method is studied in [9] to reduce error probability and improve reliability. In order to relieve the performance degradation resulted from applying conventional channel coding to URLLC short-packet transmission, a spatiotemporal 2-D channel coding scheme is proposed for very low latency reliable data transmission [10]. Enabled by the spatial freedom of massive MIMO, the proposed coding scheme in [10] can flexibly balance transmission reliability and latency for different scenarios.

In the link layer, there are also some innovative techniques to achieve URLLC, such as grant-free access, interface diversity, and radio resource allocation. Specifically, three grant-free access retransmission schemes [11] are analyzed including reactive, k-repetition, and proactive retransmission. A novel grant-free non-orthogonal multiple accessing (NOMA) scheme based on orthogonal frequency division multiplexing (OFDM) with index modulation is proposed in [12], which effectively reduces the latency in comparison to classical NOMA scheme. Considering multiuser queuing delay, radio resource management method in [13] efficiently decreases URLLC signaling overhead.

Apart from physical and link layer design, novel computing frameworks and network architecture techniques are attracting much attention. By optimizing task offloading and resource allocation at edge nodes, MEC systems shorten the delay and promise to support various mission-critical applications [14]. By serving each user with multiple links from different nodes, multi-connectivity is regarded as an effective approach to ensure high network availability and reliability [15]. To reduce control-plane latency in handover procedure, anticipatory networks predict the mobility of users according to their mobility pattern and reserve resources proactively [16].

A. Related Works

All along, packet error probability ε , blocklength (i.e. codeword size) n and coding rate R (the number of information bits per complex symbol) are the three fundamental parameters involved in communication systems. They are highly correlated to each other and no one is dispensable, just like the vertexes of a triangle. In 1948, C. E. Shannon founded the mathematical basis of communication theory and revealed that the channel capacity C is the maximal rate at which the packet error probability ε vanishes as the packet length n tends to infinity [17]. After that, through using error exponent corresponding to a fixed rate $R < C$, R. G. Gallager derived the packet error probability ε for that rate in 1965 [18]. Then, all the remainder (the last vertex of the triangle) is only about how n affects R and ε . Although this problem had already been noticed by Shannon in his early contributions, there still lacks of a unified approach to solve perfectly it [19]. Fortunately, during the last few years, significant progress has been made within the information theory community. Building upon Doobrushin's and Strassen's asymptotic results, Y. Polyanskiy, H. V. Poor and S. Verdú provided a new framework to obtain tight bounds on R as a function of n and ε , for additive white Gaussian noise (AWGN) channel [20]. The rationale behind Polyanskiy's approach is that when n is finite, the coding rate becomes a random variable composed of channel capacity and dispersion. Channel dispersion is also a random variable introduced as a rate penalty to characterize the impact of n . In the sequel, a series of works have extended their results to other kinds of point-to-point channels. In a single-input single-output (SISO), stationary coherent fading channel with additive Gaussian noise, [21] obtained a convenient two-term expression for the channel dispersion which is found to rely highly on the dynamics of the fading process. In [22], the non-asymptotic bounds of the maximum coding rate were presented which is found not to be monotonic with respect to the channel coherence time. Consequently, there exists a coherence time that will maximize the coding rate over noncoherent Rayleigh block-fading channels. Its normal approximation in the high SNR regime was then presented in [23], which provides a tractable formula for us to perform further analysis.

The use of multiple antennas for wireless communication systems has gained overwhelming interest during the last decade both in academia and industry. Multiple antennas can be utilized in order to accomplish a multiplexing gain, a diversity gain, or an antenna gain, thus enhancing the bit rate, the error performance, or the signal-to-noise-plus-interference ratio of wireless systems, eventually [7], [24], [25]. Following Polyanskiy's approach, a series of works have extended the result in single antenna to the field of multiple antennas. The maximal achievable rate of finite blocklength in quasi-static MIMO channels, under mild conditions on the fading distribution, has been provided recently by Yang *et al.* [26]. Recently, Collins in [27] obtained a channel dispersion formula for the MIMO block-fading channel where the most interesting result is that the normalized dispersion decreases with a growing number of receive antennas.

Massive MIMO was first proposed by Marzetta in 2010 [28]. Compared to traditional MIMO, massive MIMO has hundreds of antennas in base station and can then acquire more multiplexing gain and diversity gain, which improve data rate and reliability respectively. So far, massive MIMO has been adopted in 5G as a key physical-layer technology to meet the demand for higher data capacity for mobile networks. It is supposed that the massive MIMO techniques will continue to evolve and more antennas are considered to employ, as the Tera Hertz frequency band is envisioned for future 6G. More antennas would provide more augmented DoFs which leads to some remarkable properties of massive MIMO, such as channel hardening and decorrelation. That is, as the number of antennas in the system increases, the variations of channel gain decrease in both the time and frequency domain and the channel vectors become asymptotically orthogonal.

B. Main Contributions

In this paper, by exploiting Stieltjes transform, we derived the closed-form expressions for expectation and variance of channel dispersion in a massive MIMO system with ideal independent and identically distributed (*i.i.d.*) fading channels. Although the results are obtained under the assumption that the number of antennas goes to infinity, it is observed in simulations that they are also accurate for the limit number of antennas case. Most interestingly, the expectation can be further simplified to a pretty concise format in the high SNR regime, which provide a trackable way to analyze the dynamics of the MIMO channel.

Furthermore, we show that, for a MIMO systems with M transmit antennas and N receive antennas, there exists an approximate solution to general relationship among the latency n , reliability ε , desired average data rate \bar{R} and spatial DoF m , where $m = \min \{M, N\}$. The embodiment of this relationship is just a bound of the spatiotemporal 2D channel capacity which can be written by

$$\frac{\bar{R}}{m} \leq \log_2 (1 + \rho) - \sqrt{\frac{1}{mn} \Phi^{-1}(\varepsilon)} \quad (1)$$

where ρ represents the signal-to-noise ratio (SNR) and $\Phi^{-1}(\cdot)$ denotes the inverse of the Gaussian Q -function

$$\Phi(x) \triangleq \int_x^{\infty} \frac{1}{\sqrt{2\pi}} e^{-t^2/2} dt. \quad (2)$$

More interestingly, when the value of m is larger enough, it turns out to be

$$n \geq \frac{m \cdot [\Phi^{-1}(\varepsilon)]^2}{[m \log_2 (1 + \rho) - \bar{R}]^2} \propto \frac{1}{m} \quad (3)$$

which reveals an inversely proportional scaling law. That is, the latency in the time domain can be reduced by increasing some portion of the DoFs in the space domain, for the purpose of maintaining a certain level of required performance.

The paper is organized as follows. The system model and the relevant works are introduced in Section II. Section III presents a complete derivation of the expectation and variance for channel dispersion. Important results are the main content

of Section IV. Section V provides some numerical results and illustrates the application of these results to the practical low latency systems.

Notation: Boldface lower and upper case letters are used to denote vectors and matrices, respectively. The notation $(\cdot)^T$ and $(\cdot)^H$ denote the transpose and the conjugate transpose of a vector or matrix, respectively. We use \mathbf{I}_a to denote the identity matrix of size $a \times a$. The mean, variance and probability of a random variable x are illustrated by the operators $\mathbb{E}\{x\}$, $\text{Var}\{x\}$ and $\mathbb{P}\{x\}$, respectively. The notation $\mathcal{CN}(0, \sigma^2)$ represents the complex Gaussian distribution with zero mean and variance σ^2 and $\mathcal{C}^{M \times N}$ denotes complex arrays with dimension $M \times N$. Moreover, we use $\text{tr}(\mathbf{A})$ and $\det(\mathbf{A})$ to denote the trace and determinant of the matrix \mathbf{A} , respectively. Then, the Frobenius norm of a matrix \mathbf{A} is denoted by $\|\mathbf{A}\|_F \triangleq \sqrt{\text{tr}(\mathbf{A}\mathbf{A}^H)}$. At last, for two functions $f(x)$ and $g(x)$, $f(x) = \mathcal{O}(g(x))$ means that $\limsup_{x \rightarrow \infty} |f(x)/g(x)| < \infty$.

II. SYSTEM MODEL

We consider an MIMO system with M transmit antennas and N receive antennas, operating over flat fading channels. Under the assumption that the synchronization is perfect and the channel is quasi-static, the baseband equivalent discrete-time input-output relationship can be written by

$$\mathbf{Y} = \mathbf{H}\mathbf{X} + \mathbf{W}, \quad (4)$$

where $\mathbf{X} \in \mathcal{C}^{M \times n}$ is the signal transmitted over n time samples (channel uses), $\mathbf{Y} \in \mathcal{C}^{N \times n}$ is the corresponding received signal, and matrix $\mathbf{H} \in \mathcal{C}^{N \times M}$ contains the complex fading coefficients, which are random but remain constant over the n time samples. It should be noted that this assumption for channel is usually reasonable for the case of uRLLC, due to the constrain of latency. When the *i.i.d.* Rayleigh fading channel is considered, each entry of \mathbf{H} is modelled as a Gaussian variable with zero mean and unit variance. $\mathbf{W} \in \mathcal{C}^{N \times n}$ denotes the additive noise at the receiver, which is independent of \mathbf{H} and also has *i.i.d.* $\mathcal{CN}(0, 1)$ entries.

According to [26], for the case of isotropic codewords, the normal approximation of maximal achievable rate can be expressed by

$$R^*(n, \varepsilon) = C(\mathbf{H}) - \sqrt{\frac{V(\mathbf{H})}{n}} \Phi^{-1}(\varepsilon) + \mathcal{O}\left(\frac{\log n}{n}\right) \quad (5)$$

where n denotes blocklength, ε represents block error probability and $\Phi^{-1}(\cdot)$ is the inverse of the Gaussian Q -function. $C(\mathbf{H})$ and $V(\mathbf{H})$ denote the Shannon capacity and channel dispersion conditioned on \mathbf{H} . When the transmitter has no channel state information (CSI), it has been proved in [29] that the optimal power allocation should fulfill

$$\mathbf{X}\mathbf{X}^H = \frac{\rho}{M} \mathbf{I}_M. \quad (6)$$

In this case, the capacity and dispersion are further expressed as

$$C(\mathbf{H}) = \sum_{j=1}^m \log(1 + \rho\lambda_j/M) \quad (7)$$

and

$$V(\mathbf{H}) = m - \sum_{j=1}^m \frac{1}{(1 + \rho\lambda_j/M)^2} P \quad (8)$$

where λ_j denotes the j -th eigenvalue of $\mathbf{H}\mathbf{H}^H$ for $M \geq N$ and $\mathbf{H}^H\mathbf{H}$ for $M < N$.

III. STATISTICAL PROPERTIES OF CHANNEL DISPERSION

Since the channel matrix is random, its fading dynamics on the channel dispersion can be investigated by deriving its statistical properties. Specifically, its expectation, together with the capacity, can help us analyze the average maximal achievable rate. As most of the practical systems work in the positive SNR regime, we consider in this paper only the case of $\rho > 0$.

A. Expectation

Taking expectation on Eq. (8), we obtain

$$\begin{aligned} \mathbb{E}\{V(\mathbf{H})\} &= \mathbb{E}\left\{m - \sum_{j=1}^m \frac{1}{(1 + \rho\lambda_j/M)^2}\right\} \\ &= \mathbb{E}\left\{m - \sum_{j=1}^m \frac{1}{1 + 2\rho\lambda_j/M + (\rho\lambda_j/M)^2}\right\} \\ &> \mathbb{E}\left\{m - \sum_{j=1}^m \frac{1}{2\rho\lambda_j/M + (\rho\lambda_j/M)^2}\right\} \quad (9) \\ &= m - \frac{M}{2\rho} \mathbb{E}\left\{\sum_{i=1}^m \frac{1}{\lambda_i}\right\} \\ &\quad + \frac{M}{2\rho} \mathbb{E}\left\{\sum_{i=1}^m \frac{1}{2M/\rho + \lambda_i}\right\}. \end{aligned}$$

According to [30], the first expectation on the right-hand-side (RHS) of Eq. (9) can be obtained directly. That is,

i) $M > N$

$$\begin{aligned} \mathbb{E}\left\{\sum_{i=1}^m \left(\frac{1}{\lambda_i}\right)\right\} &= \mathbb{E}\left\{\text{tr}\left[\left(\mathbf{H}\mathbf{H}^H\right)^{-1}\right]\right\} \\ &= \frac{N}{M-N}, \end{aligned} \quad (10)$$

ii) $M < N$

$$\begin{aligned} \mathbb{E}\left\{\sum_{i=1}^m \left(\frac{1}{\lambda_i}\right)\right\} &= \mathbb{E}\left\{\text{tr}\left[\left(\mathbf{H}^H\mathbf{H}\right)^{-1}\right]\right\} \quad (11) \\ &= \frac{M}{N-M}. \end{aligned}$$

From Eq. (10) and (11), we can see that the sum of the reciprocals of eigenvalues is just the power of the inverse of correlation matrix. However, it is somewhat striking, that the average power does not exist when $M = N$ [31]. So, we have to add one additional antennas at transmitter to define the average power. In this case, the expectation can be expressed approximately by

$$\mathbb{E} \left\{ \sum_{i=1}^m \left(\frac{1}{\lambda_i} \right) \right\} = M - 1. \quad (12)$$

The second expectation on the RHS of Eq. (9) can be derived by using the Stieltjes transform. Stieltjes transform approach can solve most problems involved in random matrices, such as the distribution functions of the empirical eigenvalues of large random matrices [32], [33]. After some mathematical manipulations in Appendix A, we obtain its close-form expression in Eq. (13) on the top of the next page.

Fig. 1 and 2 give the simulation results for different antenna setup where $c = N/M$. The analytical results are calculated according to Eq. (13). Most interestingly, although these formulae are derived under the assumption that the number of antennas goes to infinity, their results coincide well with the simulation curve in a finite number of antennas case. Hence, we omit the limit operator in Eq. (13) for the simplicity of notation.

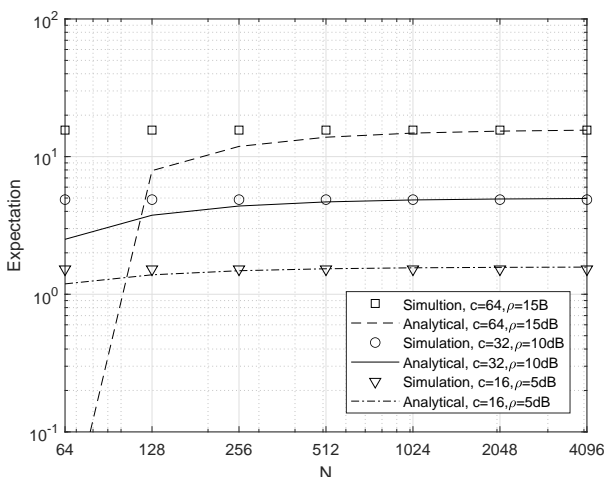


Fig. 1. Expectation comparison for $N > M$.

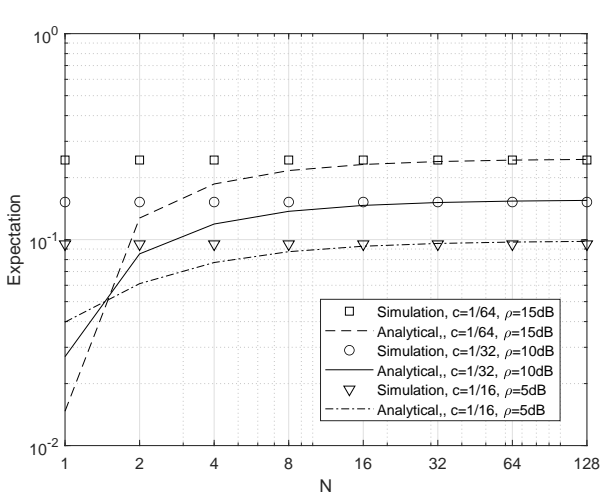


Fig. 2. Expectation comparison for $N < M$.

Finally, combining Eq. (10)-(12) and Eq. (13), we obtain the complete close-form expression for the expectation of

channel dispersion. Most Interestingly, these expressions can be further simplified to some constant in some special cases. For example, in a massive MIMO system with $N = 1$, as M goes to infinity, we find

$$\mathbb{E} \left\{ \sum_{i=1}^m \frac{1}{2M/\rho + \lambda_i} \right\} \approx 0 \quad (14)$$

and

$$\frac{M}{2\rho} \mathbb{E} \left\{ \sum_{i=1}^m \left(\frac{1}{\lambda_i} \right) \right\} = \frac{M}{2\rho} \cdot \frac{1}{M-1} \approx \frac{1}{2\rho}. \quad (15)$$

In this case, the channel dispersion, for any positive SNR, can be approximated by

$$\mathbb{E} [V(\mathbf{H})] \approx 1 - \frac{1}{2\rho}. \quad (16)$$

B. Variance

The variance of channel dispersion can be written by

$$\begin{aligned} \sigma_V^2 &= \mathbb{E} \left\{ (V(\mathbf{H}) - \mathbb{E} [V(\mathbf{H})])^2 \right\} \\ &= \mathbb{E} \left\{ \left(\sum_{j=1}^m \frac{1}{(1 + \rho \lambda_j / N_t)^2} \right)^2 \right\} \\ &\quad - \left[\mathbb{E} \left\{ \sum_{j=1}^m \frac{1}{(1 + \rho \lambda_j / N_t)^2} \right\} \right]^2 \end{aligned} \quad (17)$$

Since we already have the result of the second term of RHS in Eq. (15), the only thing left to us is to obtain the close-form formula of the first term which has a denominator of order four. Unfortunately, it is very difficult to calculate the high order moments of Wishart distributed matrices. Thus, we have to find some way to reduce the order and try to make use of the available results of low order moment. Following this idea, we approximate the first term by

$$\begin{aligned} &\mathbb{E} \left\{ \left(\sum_{j=1}^m \frac{1}{(1 + \rho \lambda_j / M)^2} \right)^2 \right\} \\ &= \mathbb{E} \left\{ \left(\sum_{j=1}^m \frac{1}{1 + 2\rho \lambda_j / M + (\rho \lambda_j / M)^2} \right)^2 \right\} \\ &> \mathbb{E} \left\{ \left(\sum_{j=1}^m \frac{1}{2\rho \lambda_j / M + (\rho \lambda_j / M)^2} \right)^2 \right\} \\ &= \mathbb{E} \left\{ \left[\frac{M}{2\rho} \sum_{i=1}^m \left(\frac{1}{\lambda_i} - \frac{1}{2M/\rho + \lambda_i} \right) \right]^2 \right\} \\ &= G1 - 2 \cdot G2 + G3 + G4. \end{aligned} \quad (18)$$

where

$$G1 = \mathbb{E} \left\{ \left(\frac{M}{2\rho} \right)^2 \sum_{i=1}^m \left(\frac{1}{\lambda_i} \right)^2 \right\}, \quad (19)$$

$$\mathbb{E} \left\{ \sum_{i=1}^m \frac{1}{2M/\rho + \lambda_i} \right\} = \begin{cases} \frac{N}{M} \left(\frac{\rho(NM-M^2)}{4N^2} - \frac{M}{2N} + \frac{\sqrt{(\rho M^2 - \rho MN + 2MN)^2 + 8\rho N^2 M^2}}{4N^2} \right) & N > M \\ \frac{\rho(NM-N^2)}{4M^2} - \frac{N}{2M} + \frac{\sqrt{(\rho N^2 - \rho MN + 2MN)^2 + 8\rho N^2 M^2}}{4M^2} & N \leq M \end{cases} \quad (13)$$

$$G2 = \mathbb{E} \left\{ \left(\frac{M}{2\rho} \right)^2 \sum_{i=1}^m \sum_{j=1}^m \frac{1}{\lambda_i (2M/\rho + \lambda_j)} \right\}, \quad (20)$$

$$G3 = \mathbb{E} \left\{ \left(\frac{M}{2\rho} \right)^2 \sum_{i=1, i \neq j}^m \frac{1}{\lambda_i \lambda_j} \right\} \quad (21)$$

and

G4 =

$$\mathbb{E} \left\{ \left(\frac{M}{2\rho} \right)^2 \sum_{i=1}^m \sum_{j=1}^m \frac{1}{(2M/\rho + \lambda_i)(2M/\rho + \lambda_j)} \right\}. \quad (22)$$

Now the original expression has been expanded to the sum of multiple parts which all have a lower order. Moreover, some of them already have close-form results. Based on the Properties of Wishart Matrices introduced in [29, Lemma 2.10], for $M > N + 1$, we have

$$G1 = \left(\frac{M}{2\rho} \right)^2 \frac{MN}{(M-N)^3 - (M-N)} \quad (23)$$

and

$$G3 = \left(\frac{M}{2\rho} \right)^2 \frac{N(N-1)}{(M-N)(M-N+1)} \quad (24)$$

Unfortunately, it is difficult to derive the exact close-form expressions for G2 and G4 by using the conventional integration approach, since there is an additional term $2M/\rho$ appearing in the denominator. So, we have to make some approximations to the original expression. Otherwise, even if it can be solved, it may comprise of some kinds of special functions which makes the expression not concise. By taking an independence assumption between two elements of G2, we obtain its close-form result, for $M > N + 1$, as

$$G2 = \zeta \left(\frac{M}{2\rho} \right)^2 \frac{N^2}{M-N} \left[\frac{N-M}{4\rho N} - \frac{1}{2} + \frac{\rho \sqrt{(M-N+2N/\rho)^2 + 8N^2/\rho}}{4N} \right], \quad (25)$$

where $\zeta = 1/(\psi N)$ denotes the emendation parameter and ψ is a real number which has different values for different ρ . *Proof:* See Appendix B.

Similar to the derivation of G2, we use the independence assumption and express G4, for the case of $M > N + 1$, as

$$G4 = \xi \left[\frac{M(N-M)}{8N} - \frac{M}{4\rho} + \frac{M \sqrt{(M-N+2N/\rho)^2 + 8N^2/\rho}}{8N} \right]^2 \quad (26)$$

where ξ is also an emendation parameter which has different values for different ρ .

IV. BOUNDS ON MAXIMAL ACHIEVABLE RATE

So far, we have achieved the close-form expressions of the expectation and variance for channel dispersion. Then, by using the Jensen's inequality, we have

$$\mathbb{E} \left[\sqrt{V(\mathbf{H})} \right] \geq \sqrt{\mathbb{E}[V(\mathbf{H})]}. \quad (27)$$

In this case, the lower bound of maximal achievable rate can be written by

$$\mathbb{E}[R^*(n, \varepsilon)] = \bar{R} \leq \mathbb{E}[C(\mathbf{H})] - \sqrt{\frac{\mathbb{E}[V(\mathbf{H})]}{n}} Q^{-1}(\varepsilon) \quad (28)$$

where the expectation of channel dispersion can be found in Eq. (10)-(13).

Although these expressions are accurate, they seems to be so complicated that it is not easy to use them in performance analysis. In fact, the results with concise expressions are more useful in studying the relationship between the blocklength and coding rate.

A. High SNR Regime

In the high SNR regime, since $\rho \gg 1$, the channel dispersion can be approximated by

$$\begin{aligned} \mathbb{E}\{V(\mathbf{H})\} &= m - \mathbb{E} \left\{ \sum_{j=1}^m \frac{1}{(1 + \rho \lambda_j/M)^2} \right\} \\ &\approx m - \frac{M^2}{\rho^2} \mathbb{E} \left\{ \sum_{j=1}^m \frac{1}{\lambda_j^2} \right\}. \end{aligned} \quad (29)$$

Based on the properties of Wishart matrices given in [32], we obtain

$$\mathbb{E}[V(\mathbf{H})] \approx m - \frac{M^2}{\rho^2} \cdot \frac{NM}{(M-N)^3 - (M-N)}. \quad (30)$$

Interestingly, as the SNR goes to infinity, Eq. (30) can be further simplified approximately to

$$\mathbb{E}[V(\mathbf{H})] \approx m. \quad (31)$$

Proof: See Appendix C.

On the other hand, the capacity in the high SNR regime also has a simple approximated formula as [25]

$$\mathbb{E}[C(\mathbf{H})] \approx m \log(1 + \rho) \quad (32)$$

Consequently, a concise and analytically trackable expression for the average coding rate at finite blocklength is achieved which can be written by

$$\bar{R} \leq m \log(1 + \rho) - \sqrt{\frac{m}{n}} \Phi^{-1}(\varepsilon). \quad (33)$$

B. Normalized Maximal Achievable Rate

As we know, after performing singular value decomposition (SVD) or eigenvalue decomposition, the MIMO channel can be transformed into multiple parallel orthogonal links. As a result, the average maximal achievable rate over all the links plays an important role in the performance analysis of massive MIMO systems at finite blocklength. Following this idea, we divide Eq. (33) by m and thus obtain

$$\frac{\bar{R}}{m} \leq \log_2(1 + \rho) - \sqrt{\frac{1}{mn}} \Phi^{-1}(\varepsilon) \quad (34)$$

which can also be viewed as the spatiotemporal 2D channel capacity. Although the potential relations of the most fundamental parameters involved in MIMO communications has been revealed in many existing results, it is the first time to describe them in a concise and accurate close-form formula. To gain a deep insight into the latency, we focus on n and m in the following analysis and let ρ and ε be any real numbers. Moreover, the channel matrix is assumed to be a square matrix with full rank, for the simplicity of analysis. In this case, from Eq. (34), we learn that the average data rate per Hz per antenna will remain unchanged, if we fix the value of mn . This fact hints that n and m can be thought of being reciprocal to some degree and thus exchanging n by m is possible in theory. In conventional MIMO systems, the channel coding is conducted in the time domain on each link independently. So, if n decreases, the reliability can not be sustained any more, for a given coding rate. However, the observed reciprocal phenomenon tells us that we can also perform channel coding in the space domain along the links and exchange n by m to keep the total performance unchanged. Indeed, when the value of m is large enough, we obtain

$$n \geq \frac{m \cdot [\Phi^{-1}(\varepsilon)]^2}{[m \log_2(1 + \rho) - \bar{R}]^2} \propto \frac{1}{m}. \quad (35)$$

which illustrates that latency is inversely proportional to the spatial DoF. This scaling law is just the basic principle behind the 2D channel coding presented in [10]. And, Eq. (35) also provides the upper bound for its maximal coding rate. More interestingly, it can be supposed that for an extreme case of $n = 1$, when m goes to infinity, the date rate per Hz per antenna, i.e. \bar{R}/m , approaches Shannon capacity.

V. NUMERICAL RESULTS AND ANALYSIS

Several computer simulations are carried out in this section to verify the correctness of the analytical results. We check the expectation of channel dispersion at first. Fig. 3 gives the simulation results for different antenna configurations where the analytical results are calculated according to Eq. (10)-(13).

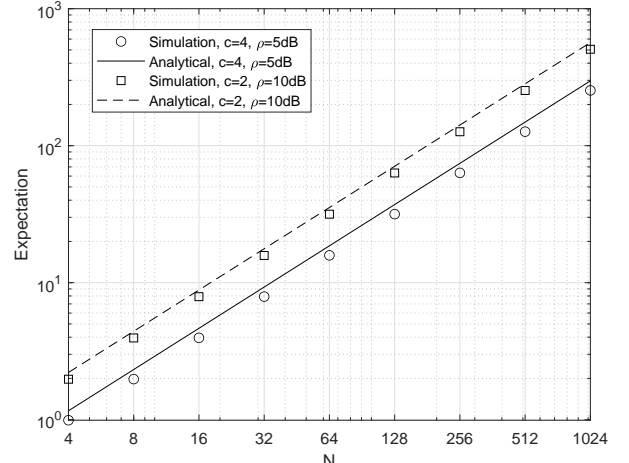


Fig. 3. Expectation of channel dispersion for $N > M$.

It should be noted, from Fig. 3, that although these results are seen to coincide well with the simulation curves, there is still a visible small gap between them. The reason is that we omit a number in the denominator of Eq. (9). Most strikingly, after analysis and simulations, we find that Eq. (36) is more accurate for whatever dimension of the matrix is used. Fig. 4 and 5 give the simulation results to demonstrate its accuracy.

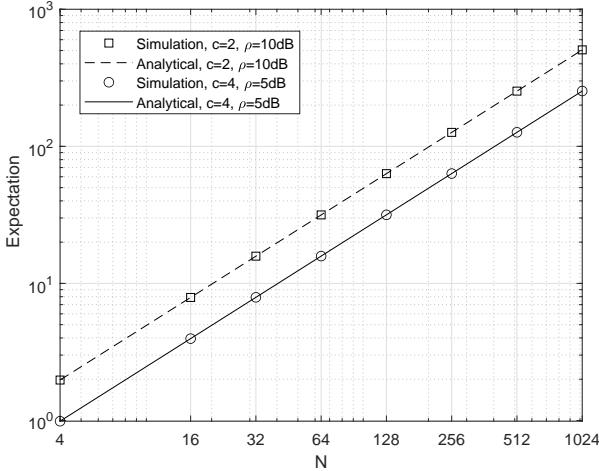
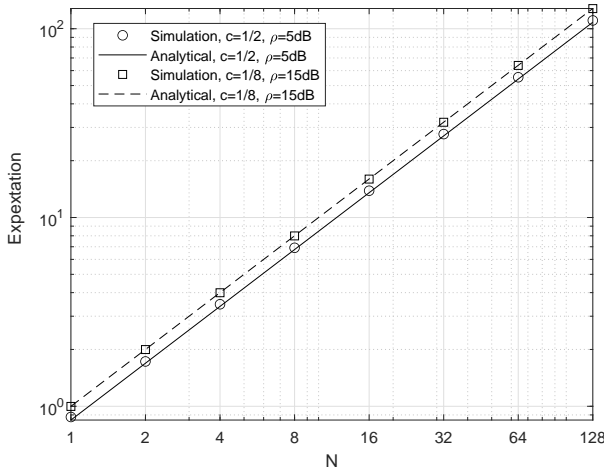
Then, we perform some simulations to see how accurate the obtained variance is. Fig. 6 illustrates the simulation results for different antenna configurations where the analytical results are calculated according to Eq. (23)-(26). The emendation parameters are set to $\psi = 1.41$ and $\xi = 0.5$ for $\rho = 5\text{dB}$ and $\psi = 1.29$ and $\xi = 0.6$ for $\rho = 7\text{dB}$. As can be seen from Fig. 6 that the variance of channel dispersion is expected to be small, when compared with the expectation, which highlights the dominant role of expectation in the analysis of system performance.

At last, some numerical results are given to expose the potential relation between blocklength and spatial DoF. Fig. 7 shows n as a function of m for the case of $\rho = 15\text{dB}$ and $\varepsilon = 10^{-7}$. For easy understanding, we set the average maximal achievable rate in Eq. (33) as a portion of capacity. Form Fig. 7, we can see that as m increases, n becomes shorter and shorter for a given rate, which illustrates the latency in the time domain can be exchanged by the antennas in the space domain.

VI. CONCLUSIONS

We have derived the closed-form expressions for channel dispersion in massive MIMO scenario, which coincide well with the simulation results. Through using the obtain channel dispersions, the bound on maximal achievable rate at finite blocklength can be expressed by a compact and precious

$$\mathbb{E}\{V(\mathbf{H})\} = \begin{cases} M - \frac{M^2}{2\rho(N-M)} + \frac{M^2}{2\rho N} \left(\frac{\rho(NM-N^2)}{4M^2} - \frac{N}{2M} + \frac{\sqrt{(\rho N^2 - \rho MN + 2MN)^2 + 8\rho N^2 M^2}}{4M^2} \right) & N > M \\ N - \frac{MN}{2\rho(M-N)} + \frac{N}{2\rho} \left(\frac{\rho(NM-M^2)}{4N^2} - \frac{M}{2N} + \frac{\sqrt{(\rho M^2 - \rho MN + 2MN)^2 + 8\rho N^2 M^2}}{4N^2} \right) & N \leq M \end{cases} \quad (36)$$

Fig. 4. Expectation of channel dispersion for $N > M$.Fig. 5. Expectation of channel dispersion for $N < M$.

formula in a normal approximation case which forms an unified framework to explore the relations among ϵ , n , R and the number of spatial DoF. Based on the new framework, it is proved at the first time that, although most people think it is intuitively reasonable, coding along the space domain can also achieve the Shannon capacity, when the number of antennas goes to infinity. This gives rise a new methodology, named time-space shifting, to solve the contradictory problem between data rate and time latency.

APPENDIX

A. Proof of Eq. (13)

Let $\mathbf{\Lambda}$ be a diagonal matrix of eigenvalues of \mathbf{R} , where $\mathbf{R} = \mathbf{H}^H \mathbf{H}$ for the case of $N > M$. According to the definition of

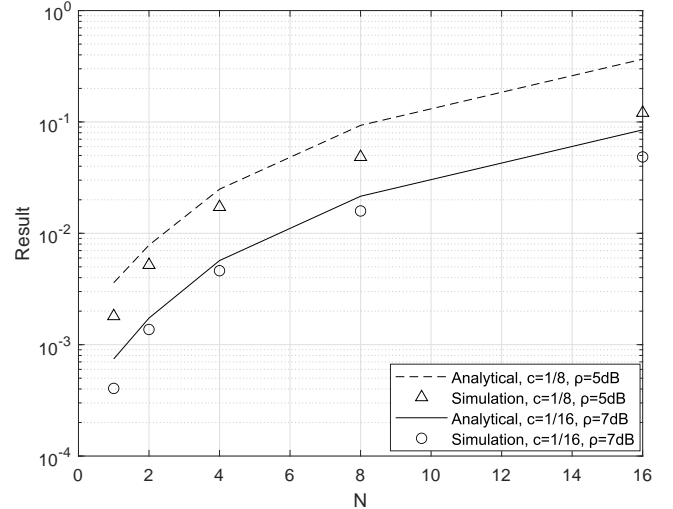


Fig. 6. Comparison of analytical and simulation results.

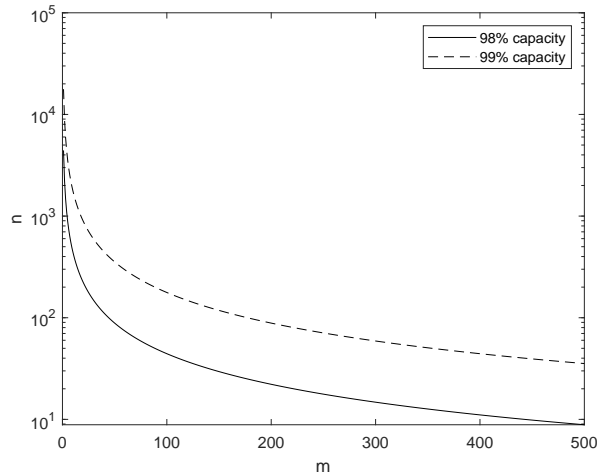


Fig. 7. Comparison of locklength for different DoFs.

Stieltjes transform in [33], we have

$$\begin{aligned} \sum_{i=1}^m \frac{1}{2M/\rho + \lambda_i} &= \text{tr} \left[(\mathbf{\Lambda} - z\mathbf{I}_m)^{-1} \right] \\ &= m \int \frac{1}{\lambda - z} dF^{\mathbf{R}}(\lambda), \end{aligned} \quad (37)$$

where $F^{\mathbf{R}}$ denotes the eigenvalue distribution function of \mathbf{R} and $z = -2M/\rho$. When m grows to infinity, it has been proved that $F^{\mathbf{R}}$ converges in distribution (often almost surely so) to some deterministic limit F , which can then be turned into approximative results for $F^{\mathbf{R}}$. Furthermore, by using Marčenko-Pastur law, the Stieltjes transform has a explicit

expression as

$$\mu_F(z) = \frac{1-c}{2cz} - \frac{1}{2c} - \frac{\sqrt{(1-c-z)^2 - 4cz}}{2cz} \quad (38)$$

where $c = N/M$. Nevertheless, it should be noted that the entries of the matrices dealt with in this law have different variances with that of the elements in \mathbf{H} . So, the result of Eq. (38) should be scaled. Based on [32, Lemma 3.2], i.e.,

$$\mu_{a\mathbf{R}}(az) = \frac{1}{a}\mu_{\mathbf{R}}(z), \quad (39)$$

we obtain

$$\mu_F(z) = a \left(\frac{1-c}{2caz} - \frac{1}{2c} - \frac{\sqrt{(1-c-az)^2 - 4caz}}{2caz} \right) \quad (40)$$

where $a = c/M$. Since all the variables in this expression are deterministic, we say that the expectation approaches to

$$\lim_{M \rightarrow \infty} \mathbb{E} \left\{ \sum_{i=1}^m \frac{1}{2M/\rho + \lambda_i} \right\} = c \left(\frac{1-c}{2caz} - \frac{1}{2c} - \frac{\sqrt{(1-c-az)^2 - 4caz}}{2caz} \right). \quad (41)$$

Finally, substituting $c = N/M$, $a = c/M$ and $z = -2M/\rho$ into Eq. (41) yields Eq. (13).

On the other hand, when $N \leq M$, Eq. (38) still holds. So, as long as we set $c' = 1/c$ and $a' = c'/M$ to scale the matrix, the expectation can then be obtained as

$$\lim_{M \rightarrow \infty} \mathbb{E} \left\{ \sum_{i=1}^m \frac{1}{2M/\rho + \lambda_i} \right\} = \left(\frac{1-c'}{2c'a'z} - \frac{1}{2c'} - \frac{\sqrt{(1-c'-a'z)^2 - 4c'a'z}}{2c'a'z} \right) \quad (42)$$

where $z = -2M/\rho$.

B. Proof of Eq. (25)

If all the eigenvalues are independent of each other, we can rewrite Eq. (20) as

$$\mathbb{E} \left\{ \left(\frac{M}{2\rho} \right)^2 \sum_{i=1}^m \sum_{j=1}^m \frac{1}{\lambda_i (2M/\rho + \lambda_j)} \right\} = \left(\frac{M}{2\rho} \right)^2 \mathbb{E} \left\{ \sum_{i=1}^m \frac{1}{\lambda_i} \right\} \mathbb{E} \left\{ \sum_{j=1}^m \frac{1}{2M/\rho + \lambda_j} \right\}. \quad (43)$$

Then, by using the results in Eq. (10) and (13), it is easy to obtain

$$\begin{aligned} & \left(\frac{M}{2\rho} \right)^2 \mathbb{E} \left\{ \sum_{i=1}^m \frac{1}{\lambda_i} \right\} \mathbb{E} \left\{ \sum_{j=1}^m \frac{1}{2M/\rho + \lambda_j} \right\} \\ &= \left(\frac{M}{2\rho} \right)^2 \frac{N^2}{M-N} \left[\frac{N-M}{4\rho N} - \frac{1}{2} \right. \\ & \quad \left. + \frac{\rho \sqrt{(M-N+2N/\rho)^2 + 8N^2/\rho}}{4N} \right]. \end{aligned} \quad (44)$$

However, we all know that the eigenvalues are not independent in a matrix. They are actually correlated to each other. So, this expression is not accurate and needs to be emended. Fortunately, simulation results show that it has the same trend of variation as that of G2 and their difference can be corrected by a constant parameter. Thus, we finally obtain

$$\begin{aligned} G2 = \zeta \left(\frac{M}{2\rho} \right)^2 \frac{N^2}{M-N} \left[\frac{N-M}{4\rho N} - \frac{1}{2} \right. \\ & \quad \left. + \frac{\rho \sqrt{(M-N+2N/\rho)^2 + 8N^2/\rho}}{4N} \right] \end{aligned} \quad (45)$$

where $\zeta = 1/(\psi N)$ denotes the emendation parameter and ψ is a real number which has different values for different ρ .

C. Proof of Eq. (31)

At first, we consider $M > N$ and obtain

$$\begin{aligned} \mathbb{E}[V(\mathbf{H})] & \approx m - \frac{m}{\rho^2} \cdot \frac{M^3}{(M-m)^3 - (M-m)} \\ &= m \left(1 - \frac{1}{\rho^2} \cdot \frac{M^3}{(M-m)^3 - (M-m)} \right) \\ &= m \left(1 - \frac{1}{\rho^2} \cdot G6 \right). \end{aligned} \quad (46)$$

In practical systems, the number of transmit antennas is usually set to be an integer multiple of the receive antennas, such as 5G downlink, to facilitate the use of multi-user MIMO or support coordinated multiple points (CoMP) transmissions. In this case, M is an even number and m ranges from 1 to $M/2$, i.e., $1 \leq m \leq M/2$. Substituting the extreme values into G6 and assuming $M > 2$, we obtain

$$\begin{aligned} \frac{M^3}{(M-m)^3 - (M-m)} & < \frac{M^3}{\left(M - \frac{M}{2} \right)^3 - (M-1)} \\ &= \frac{8M^2}{M^2 - 8 + \frac{8}{M}} < 13. \end{aligned} \quad (47)$$

In the high SNR regime, ρ is of course larger than $\sqrt{13}$. So,

$$\frac{1}{\rho^2} \cdot G5 < 1 \quad (48)$$

holds obviously. When we further increase ρ to a very large number, the term in Eq.(46) diminishes completely and Eq. (31) is obtained then.

For the case of $M < N$, the bound of ρ to make G5 be smaller than one can be found by using the same way, but we would not repeat it here, due to the limited room.

REFERENCES

- [1] J. Sachs, G. Wikstrom, T. Dudda, et al., “5G radio network design for ultra-reliable low-latency communication,” *IEEE Network*, vol. 32, no. 2, pp. 24–31, 2018.
- [2] S. Liu, C. Zheng, Y. Huang, and T. Q. S. Quek, “Distributed reinforcement learning for privacy-preserving dynamic edge caching,” *IEEE Journal on Selected Areas in Communications*, vol. 40, no. 3, pp. 749–760, 2022.
- [3] 3rd Generation Partnership Project (3GPP), *Evolved Universal Terrestrial Radio Access (E-UTRA); Radio Resource Control (RRC); Protocol specification*, Technical Specification (TS) 36.331, 04 2017.
- [4] G. J. Sutton, J. Zeng, R. P. Liu, et al., “Enabling technologies for ultra-reliable and low latency communications: From PHY and MAC layer perspectives,” *IEEE Communications Surveys Tutorials*, vol. 21, no. 3, pp. 2488–2524, 2019.
- [5] X. You, Y. Huang, S. Liu, et al., “Toward 6G TKμ extreme connectivity: Architecture, key technologies and experiments,” submitted to *IET Networks*, 2022.
- [6] W. Saad, M. Bennis, and M. Chen, “A vision of 6G wireless systems: Applications, trends, technologies, and open research problems,” *IEEE Network*, vol. 34, no. 3, pp. 134–142, 2019.
- [7] X. You, C. Wang, J. Huang, et al., “Towards 6G wireless communication networks: Vision, enabling technologies, and new paradigm shifts,” *Science China Information Sciences*, vol. 64, no. 1, pp. 1–74, 2021.
- [8] H. Ren, C. Pan, Y. Deng, M. Elkashlan, and A. Nallanathan, “Joint pilot and payload power allocation for massive-MIMO-enabled URLLC IIoT networks,” *IEEE Journal on Selected Areas in Communications*, vol. 38, no. 5, pp. 816–830, May 2020.
- [9] Y. Xie, P. Ren and D. Xu, “Transmission performance optimization for URLLC with limited training and feedback overheads,” *IEEE Access*, vol. 8, pp. 140467–140477, 2020.
- [10] X. You, C. Zhang, B. Sheng, Y. Huang, C. Ji, Y. Shen, W. Zhou and J. Liu, “Spatiotemporal 2-D channel coding for very low latency reliable MIMO transmission,” *arXiv preprint*, arXiv:2201.03166.
- [11] Y. Liu, Y. Deng, M. Elkashlan, A. Nallanathan, and G. K. Karagiannidis, “Analyzing grant-free access for URLLC service,” *IEEE Journal on Selected Areas in Communications*, vol. 39, no. 3, pp. 741–755, Mar. 2021.
- [12] S. Dogan, A. Tusha and H. Arslan, “NOMA with index modulation for uplink URLLC through grant-free access,” *IEEE Journal of Selected Topics in Signal Processing*, vol. 13, no. 6, pp. 1249–1257, Oct. 2019.
- [13] C. She, C. Yang and T. Q. S. Quek, “Radio resource management for ultra-reliable and low-latency communications,” *IEEE Communications Magazine*, vol. 55, no. 6, pp. 72–78, June 2017.
- [14] C. She, Y. Duan, G. Zhao, T. Q. S. Quek, Y. Li and B. Vucetic, “Cross-layer design for mission-critical IoT in mobile edge computing systems,” *IEEE Internet of Things Journal*, vol. 6, no. 6, pp. 9360–9374, Dec. 2019.
- [15] C. She, Z. Chen, C. Yang, T. Q. S. Quek, Y. Li and B. Vucetic, “Improving network availability of ultra-reliable and low-latency communications with multi-connectivity,” *IEEE Transactions on Communications*, vol. 66, no. 11, pp. 5482–5496, Nov. 2018.
- [16] N. Bui, M. Cesana, S. A. Hosseini, Q. Liao, I. Malanchini and J. Widmer, “A survey of anticipatory mobile networking: Context-based classification, prediction methodologies, and optimization techniques,” *IEEE Communications Surveys & Tutorials*, vol. 19, no. 3, pp. 1790–1821, Q3 2017.
- [17] C. E. Shannon, “A mathematical theory of communication,” *Bell System Technical Journal*, vol. 27, pp. 379–423, 1948.
- [18] R. G. Gallager, *Information theory and reliable communication*, New York, USA, Wiley, 1968.
- [19] X. You, “Shannon theory and future 6G’s technique potentials,” *Scientia Sinicae Informationis*, vol. 50, no. 9, pp. 1377–1394, 2020.
- [20] Y. Polyanskiy, H. V. Poor, and S. Verdú, “Channel coding rate in the finite blocklength regime,” *IEEE Trans. Inf. Theory*, vol. 56, no. 5, pp. 2307–2359, May 2010.
- [21] Y. Polyanskiy and S. Verdú, “Scalar coherent fading channel: Dispersion analysis,” in *Proceedings of the IEEE International Symposium on Information Theory*, pp. 2959–2963, Aug. 2011.
- [22] W. Yang, G. Durisi, T. Koch, and Y. Polyanskiy, “Diversity versus channel knowledge at finite block-length,” in *Proceedings of the IEEE Information Theory Workshop*, pp. 572–576, Sept. 2012.
- [23] A. Lancho, T. Koch, and G. Durisi, “On single-antenna Rayleigh block-fading channels at finite blocklength,” *IEEE Trans. Inf. Theory*, vol. 66, no. 1, pp. 496–519, Jan. 2020.
- [24] E. Telatar, “Capacity of multi-antenna Gaussian channels,” *European Trans. Telecommun.*, vol. 10, no. 6, pp. 585–595, Dec. 1999.
- [25] L. Zheng and D. Tse, “Diversity and multiplexing: A fundamental tradeoff in multiple-antenna channels,” *IEEE Trans. Inf. Theory*, vol. 49, no. 5, pp. 1073–1096, May 2003.
- [26] W. Yang, G. Durisi, T. Koch, and Y. Polyanskiy, “Quasi-static multiple-antenna fading channels at finite blocklength,” *IEEE Trans. Inf. Theory*, vol. 60, no. 7, pp. 4232–4265, Jul. 2014.
- [27] A. Collins and Y. Polyanskiy, “Dispersion of the coherent MIMO block-fading channel,” in *Proceedings of the IEEE International Symposium on Information Theory (ISIT)*, 2016, Barcelona, Spain, pp. 572–576.
- [28] T. L. Marzetta, “Noncooperative cellular wireless with unlimited numbers of base station antennas,” *IEEE Trans. Wireless Commun.*, vol. 9, no. 11, pp. 3590–3600, Nov. 2010.
- [29] E. Abbe, S.-L. Huang, and I. E. Telatar, “Proof of the outage probability conjecture for MISO channels,” *IEEE Trans. Inf. Theory*, vol. 59, no. 5, pp. 2596–2602, May 2013.
- [30] A. Lozano, A. M. Tulino, and S. Verdú, “Multiple-antenna capacity in the low-power regime,” *IEEE Trans. Inf. Theory*, vol. 49, no. 10, pp. 2527–2544, Oct. 2003.
- [31] V. Jungnickel, T. Haustein, E. Jorswieck, and C. von Helmolt, “On linear pre-processing in multi-antenna systems,” in *Proc. IEEE GLOBECOM*, Taiwan, China, pp. 1012–1016, Nov. 2002.
- [32] A. M. Tulino and S. Verdú, *Random matrix theory and wireless communications*, Now Foundations and Trends, 2004.
- [33] R. Couillet and M. Debbah, *Random matrix methods for wireless communications*, Cambridge University Press, 2011.